Entanglement-based quantum communication over 144 km

R. URSIN[1]*, F. TIEFENBACHER[1,2], T. SCHMITT-MANDERBACH[3,4], H. WEIER[4], T. SCHEIDL[1,2], M. LINDENTHAL[2], B. BLAUENSTEINER[1], T. JENNEWEIN[2], J. PERDIGUES[5], P. TROJEK[3,4], B. ÖMER[6], M. FÜRST[4], M. MEYENBURG[6], J. RARITY[7], Z. SODNIK[5], C. BARBIERI[8], H. WEINFURTER[3,4] AND A. ZEILINGER[1,2]*

[1]Institute for Experimental Physics, University of Vienna, A-1090 Vienna, Austria
[2]Institute for Quantum Optics and Quantum Information, Austrian Academy of Sciences, A-1090 Vienna, Austria
[3]Max-Planck-Institut für Quantenoptik, D-85748 Garching, Germany
[4]Department für Physik, Ludwig-Maximilians University, D-80799 Munich, Germany
[5]European Space Agency, 2200 AG Noordwijk, The Netherlands
[6]Business Unit Quantum Technology, ARC Seibersdorf Research GmbH, A-1220 Vienna, Austria
[7]Department of Electrical and Electronic Engineering, University of Bristol, Bristol, BS8 1UB, UK
[8]Department of Astronomy, University of Padova, I-35122, Italy
*e-mail: Rupert.Ursin@univie.ac.at; Zeilinger-office@quantum.at

Published online: 3 June 2007; doi:10.1038/nphys629

Quantum entanglement is the main resource to endow the field of quantum information processing with powers that exceed those of classical communication and computation. In view of applications such as quantum cryptography or quantum teleportation, extension of quantum-entanglement-based protocols to global distances is of considerable practical interest. Here we experimentally demonstrate entanglement-based quantum key distribution over 144 km. One photon is measured locally at the Canary Island of La Palma, whereas the other is sent over an optical free-space link to Tenerife, where the Optical Ground Station of the European Space Agency acts as the receiver. This exceeds previous free-space experiments by more than an order of magnitude in distance, and is an essential step towards future satellite-based quantum communication and experimental tests on quantum physics in space.

Entangled particles[1,2] shared between two distant observers can be used in quantum cryptography to establish an unconditional secure key[3–5], in quantum teleportation[6–10] to transfer quantum information, and are also an important ingredient for quantum computation[9,11–13]. The question arises of whether quantum entanglement can be used in communication protocols even over global distances. Up to now, this has been verified over distances of up to 13 km (refs 14–18) using polarization-entangled photons via free-space links through the atmosphere. For time-bin entanglement a 10 km link was demonstrated in optical fibres[19] and a laboratory experiment was carried out in coiled fibre[20,21] over 105 km. In order to go well beyond all the existing tests, it is necessary to significantly expand the distance between the observers measuring the entangled particles. On the basis of present fibre and detector technology, it has been determined that absorptive losses and the dark count of the detectors limit the distance for distributing entanglement to the order of 100 km (ref. 22). One approach to overcome this limitation is the implementation of quantum repeaters, which, however, still need significant development[23]. Another approach is using free-space links, involving satellites in space for bridging distances on a global scale and eventually establishing a worldwide quantum communication network[24]. Here we report an experiment where we were able to generate a quantum cryptographic key over 144 km by exploiting the randomness and the strong correlations inherent in quantum entanglement. This experiment demonstrates a first important step towards future satellite-based distribution of entangled photons to two different ground stations to establish a worldwide network for quantum communication[25] and fundamental tests of quantum physics. A schematic layout of the experimental set-up on the Canary Islands is shown in Fig. 1. Polarization-entangled photon pairs were generated on Roque de los Muchachos (2,392 m above sea level) on the island of La Palma. A picosecond-pulsed Nd:vanadate laser emitting light at 355 nm wavelength, with a repetition rate of 249 MHz and an average power of 150 mW, pumped a β-barium-borate crystal in a type-II scheme of spontaneous parametric down-conversion[26]. The source produced polarization-entangled photon pairs close to the singlet state

$$|\Psi^-\rangle = \frac{1}{\sqrt{2}}(|\mathrm{H}\rangle_\mathrm{A}|\mathrm{V}\rangle_\mathrm{B} - |\mathrm{V}\rangle_\mathrm{A}|\mathrm{H}\rangle_\mathrm{B}),$$

where H and V represent horizontally and vertically polarized photon states respectively, and the subscripts A and B label the spatial modes.

In the singlet state the polarization-measurement results are (anti-) correlated in any basis. The photons were coupled into single-mode optical fibres selecting energy-degenerate pairs of entangled photons with a wavelength of 710 nm and a bandwidth of 3 nm. When detecting both photons locally, we were able to

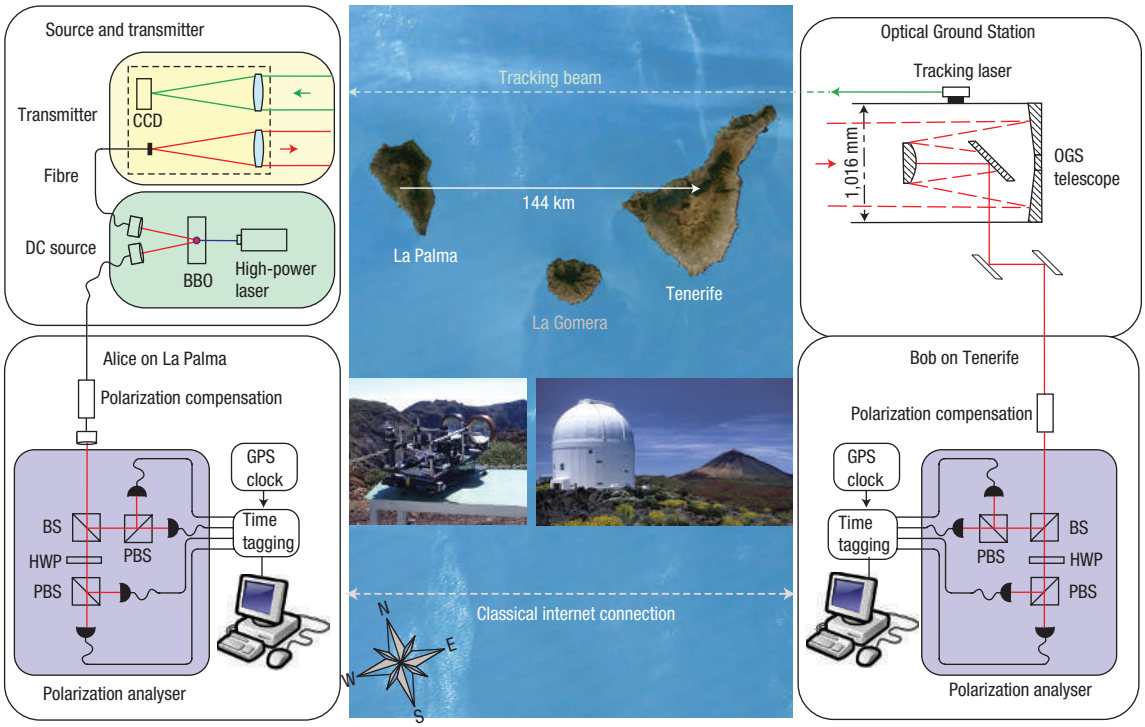

Figure 1 The free-space link between the Canary Islands La Palma and Tenerife in a picture taken from a satellite (clouds are shown here). Polarization-entangled photon pairs were produced in a type-II parametric down-conversion (DC) source by pumping a β-barium-borate crystal (BBO) with a high-power ultraviolet laser. One photon was measured locally on La Palma; the other one was sent through a 15 cm transceiver lens over the 144 km free-space optical link to the 1 m mirror telescope of the Optical Ground Station (OGS) on the island of Tenerife. The link was actively stabilized by analysing the direction of a tracking beam (532 nm) sent from OGS to La Palma, which was received in a second lens focusing it on a CCD (see Fig. 2). No optical cross-talk occurred in the quantum channel, because the tracking laser was sent in the opposite direction; additionally, interference filters were used. Both parties were using four-channel polarization analysers, consisting of a 50/50 beam-splitter (BS), a half-wave plate (HWP) and two polarizing beam-splitters (PBS), which analysed the polarization of an incident photon either in the H/V or in the $+/-45^{\circ}$ basis, randomly split by the BS. Time-tagging units were used to record the individual times at which each detection event occurred relative to a timescale disciplined by the GPS. Already during data taking, Bob transmitted his time tags via a public internet channel to Alice. She found the coincident photon pairs in real time by maximizing the cross-correlation of these time tags using fast time-correlation software.

observe single count rates of 1 million counts per second (Mcps) each, and 145,000 coincident events per second. The probability of an emission of a second photon pair per pump pulse was 0.026. This reduced the visibility of the pair correlations by 1.3% because the polarizations of the two pairs are uncorrelated[27]. We finally observed polarization correlations in the H/V basis with a visibility of 98%, and in the $+45^{\circ}/-45^{\circ}$ basis with a visibility of 96%. Thus, for the first time, a source of high-quality polarization-entangled photons, capable of achieving the coincidence production rate required for a space experiment, could be used[28]. One photon from the entangled pair was measured locally (Alice). The second photon was sent via a single-mode fibre to a transmitter telescope. There, the beam was guided via a 150-mm-diameter lens with 400 mm focal length ($f/2.7$) matching the divergence of the optical fibre over a 144-km-long free-space link to Bob in the Optical Ground Station (OGS) of the European Space Agency (ESA) on Tenerife, 2,410 m above sea level[29].

Due to various atmospheric influences such as changes of the atmospheric layering and temperature and humidity gradients, the apparent bearing of the receiver station varied on timescales of tens of seconds to minutes. Accordingly, vertical movements seemed to be more pronounced than horizontal ones (see Fig. 2a). Most classical optical communication channels prevent the beam from drifting off the receiver aperture by defocusing the beam. This is not an option in single-photon experiments, where maintaining the maximum link efficiency is essential. Hence in our experiment the alignment of the transmitter telescope was controlled automatically by a closed-loop tracking system using a 532 nm beacon laser shining from the OGS to the single-photon transmitter[30,31] (see the Methods section). Besides these beam drifts, further processes led to an attenuation of the optical link: beam spreading loss due to diffraction, absorption of the atmosphere and losses due to imperfections of optical components in the set-up. Atmospheric losses were expected to be around 0.07 dB km^{-1} at these altitudes[32–34]. In addition, effects due to atmospheric turbulence, such as beam wander, rapidly evolving speckle patterns and turbulence-induced beam spreading, caused losses (see below). All these losses reduced the link efficiency but did not affect the polarization.

The OGS (Bob), a 1 m Richey-Chrétien/Coudé telescope (see Fig. 1) with an effective focal length of 39 m ($f/39$), was used to collect the single photons with a field of view of 8 arcmin. The atmospheric turbulence caused significant beam wander in the focal plane of the telescope of up to 3 mm in the worst case. Analysing this beam wander by taking time-averaged images on a CCD (charge-coupled device) camera we obtained a Fried parameter r_0. This corresponds to the aperture that has the 'same resolution' as a diffraction-limited aperture in the absence of turbulence[35]. This varied between $r_0 = 1$ cm in poor conditions and $r_0 = 6$ cm in best case conditions, corresponding to angular

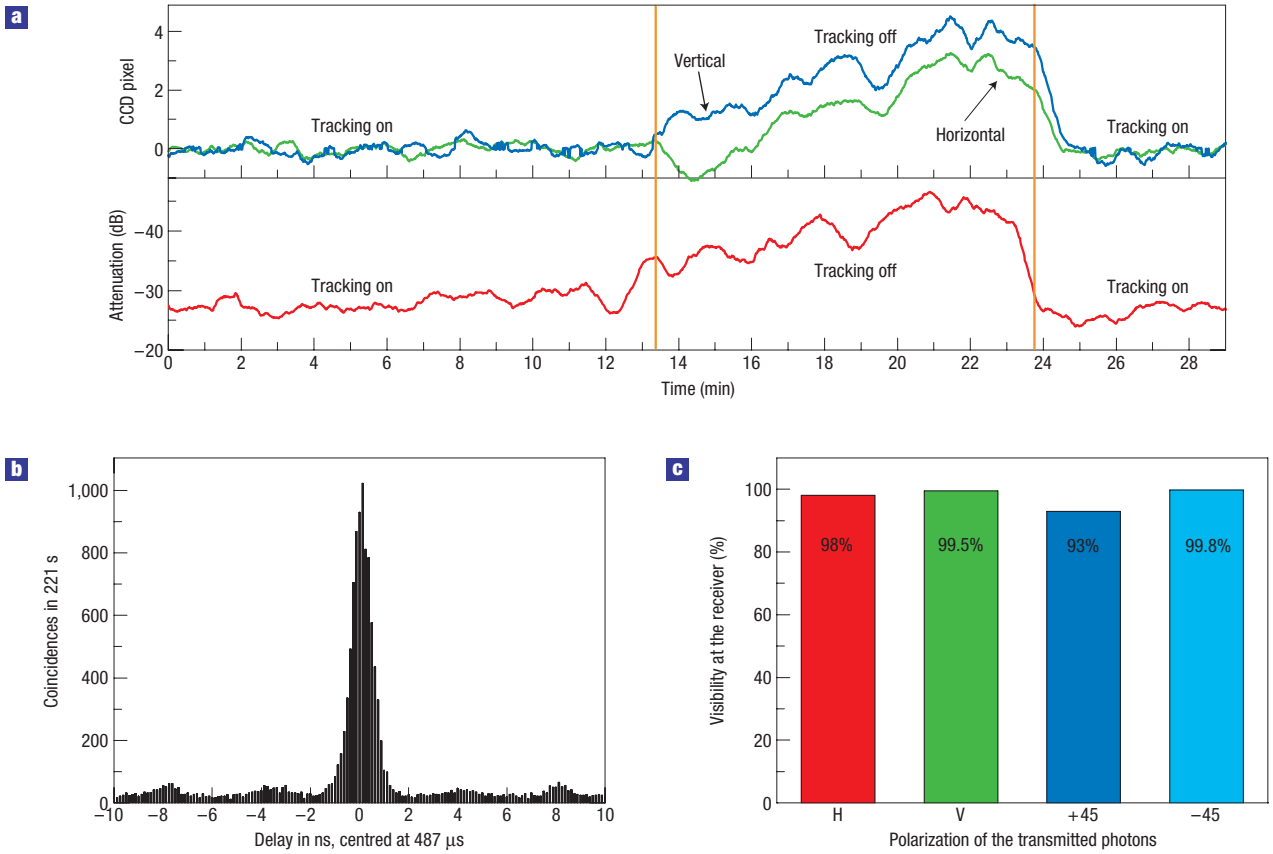

Figure 2 Complete characterization of the quantum link. a, The power received at the OGS Coudé focus from a test laser at 808 nm and the deviation of the tracking laser sampled by the CCD camera (4.5 μm pixel size) of the transmitter telescope as a function of time. Slow changes in average pointing direction occurred during changes of the atmospheric temperature gradients and layering. To maintain maximum link efficiency over the quantum link the alignment of the transmitter platform was controlled automatically by a closed-loop tracking system. A 532 nm beacon laser sent from the OGS to the transmitter was focused onto a CCD camera attached to the optical platform of the transmitter. The tracking laser was sent in the opposite direction to the quantum channel; hence no cross-talk occurred in the quantum channel. The beam drifts were compensated by keeping the spot of the tracking laser on a fixed reference position by permanently readjusting the transmitter platform. Without tracking (tracking off), the beam drifted off the receiving telescope and the transmitted power decreased accordingly. **b**, The distribution of occurrences of the coincidences between Alice's and Bob's detections with a timing resolution of 156 ps. Centred around the flight time from Alice to Bob of about 487 μs, a clear peak occurs owing to the entangled photons arriving within the coincidence window of 0.8 ns. The side peaks occurring with a period of 4 ns are due to the pulsed nature of our entangled photon source (249 MHz). This feature was used in our data analysis; detector clicks between the pulses were suppressed and not used, improving the fidelity of the results. **c**, This diagram shows the visibilities obtained using a polarized test laser beam at 808 nm wavelength transmitted over the 144 km link. The polarization was measured in the four-channel polarization analyser in the OGS Coudé focus in a time interval of 10 min after polarization compensation. The residual visibility is shown and is constant. This shows that any polarization drifts and depolarizing effects can be ignored here.

beam wander between 13 and 73 μrad ($1/e^2$ radii) and effective beam diameters at the OGS of 3.6–20 m. In the diffraction-limited case, the transmitter telescope would produce a beam of 1.5 m in diameter. To prevent the beam from wandering off the detectors we re-collimated with an additional $f = 400$ mm lens to pass through the polarization analyser and a 10-nm-full-width-at-half-maximum filter. Finally the single photons were focused with $f = 50$ mm lenses onto Si avalanche photodiodes. The resulting beam size and beam wander were smaller than the detector's active area of 500 μm in diameter. We measured a link efficiency for single photons of −25 dB under best conditions and typically −30 dB (Fig. 2a). From this we estimate between −8 and −12 dB to be due to atmospheric loss, and between −10 and −16 dB due to beam spreading wider than the aperture of the receiver telescope. Optical components in the OGS Coudé focus together with the output lens of the transmitter telescope accounted for −2 dB attenuation. Finally, our detector system (including the polarization analyser) had a quantum efficiency of ∼25% equivalent to a further −6 dB of loss. From the single photons transmitted at night-time from the source to the OGS we observed 120 cps in each of our four detectors and some 50 cps collected from background photons per detector. Together with the detector dark counts, 200 cps per detector, a total count rate of 1,500 cps is recorded. Each event in one of Alice's or Bob's detectors (see Fig. 1) was locally labelled with a 64-bit tag, containing the detector channel and a time tag with a timing resolution of 156 ps. The local clocks of the time-tagging system were 10 MHz oscillators directly disciplined by the global positioning system (GPS) with a relative drift of less than 10^{-11} over 100 s. Furthermore, the 1 Hz GPS synchronization provided a time reference for Alice's and Bob's time tags and the network timing protocol was used to initiate the time tagging within 500 ms for both parties. Bob sent his time-tag data to Alice via the public internet. Alice identified the coincident events by cross-correlating both sets of time tags using software that determined the offset

Table 1 Experimental results. We experimentally determined the polarization correlation coefficients to test the violation of a Clauser–Horne–Shimony–Holt-(CHSH-) type Bell inequality[36] to verify the integrity of our quantum communication channel. Combining our experimental data, we obtained the value of $S_{Exp} = 2.508 \pm 0.037$, thereby conclusively proving the presence of entanglement between the photons detected at the Canary Islands La Palma and Tenerife. The counting statistics accumulated within the measurement time of 221 s leads to a violation of S by 13 standard deviations.

Φ_A, Φ_B	0°, 22.5°	0°, 67.5°	45°, 22.5°	45°, 67.5°
$E(\Phi_A, \Phi_B)$	-0.775 ± 0.015	0.486 ± 0.020	-0.435 ± 0.023	-0.812 ± 0.014

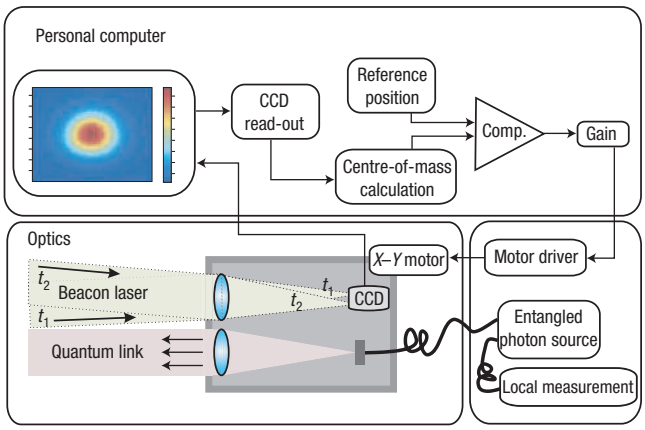

Figure 3 The closed-loop tracking system on La Palma. This consists of an optical telescope (optics) capable of transmitting single photons (quantum link) and receiving a beacon laser simultaneously. The received beacon enters the tracking lens with a time-dependent angle of arrival, hitting the CCD camera at different positions. This position was read out by a computer and compared with a previous defined reference position. The calculated error signal was used to readjust the telescope with the single-photon transmitter terminal pointing direction (*X*–*Y* motor).

(~487 μs) and drift of the two timescales. Within a coincidence window of about 1 ns, the average coincidence count rate was about 20–40 cps, depending on the actual atmospheric conditions.

To ensure the integrity of our quantum communication channel, we experimentally verified the presence of entanglement between measurement results on La Palma and Tenerife by evaluating the CHSH inequality[36] from a particular set of polarization correlations $E(\Phi_A, \Phi_B)$ (see Table 1), the 'Bell parameter' S. For perfectly entangled quantum states quantum-mechanical predictions violate this limit with a maximum value of $2\sqrt{2} \cong 2.828$ (for details see the Methods section). In our experiment, typically measuring over a time of 221 s with 7,058 coincidence events in total, we found $S = 2.508 \pm 0.037$, demonstrating the violation of the CHSH inequality by more than 13 standard deviations without any background subtraction. This violation provides evidence of entanglement between the photons observed 144 km apart, and therefore the security of a quantum key exchange on the basis of the Ekert protocol[3], where the S parameter is a measure of the information an eavesdropper could have gained on the key.

To further demonstrate the applicability of our set-up for quantum communication, we used the quantum entanglement between our pairs to actually generate a quantum cryptographic key[37]. In the experiment, we aligned the polarization compensators at the source for maximum singlet anticorrelations in the H/V and +/− bases. These settings yielded 789 coincidences within 75 s (Fig. 2). The data set was used for quantum key distribution implemented on Alice's and Bob's computers starting from 417 bits of raw key with 20 erroneous bits, which corresponds to a qubit bit error ratio of 4.8% ± 1% explicable by the various imperfections of our experimental set-up (see Fig. 2). Error correction was implemented using the CASCADE algorithm[38]. Privacy amplification[39] was done via a universal-2-class hash function with Toeplitz matrices[40,41], assuming all errors are owing to an eavesdropper attack. We finally obtained a secure key with a length of 178 bits in total[42] (note that owing to the limited statistics of our data a higher information leakage as given from the qubit bit error ratio could be considered). The alignment of the quantum communication system used up most of the available link time; the measurement time for the quantum communication was therefore limited.

Note that entangled photon pairs are definitely favourable to heralded single photons for quantum cryptography. One reason is the reduced information leakage in the case of double pair emission. Entanglement between four photons exists only if they are emitted within the coherence time (about 100 fs in our case); all other instances have to be treated as emission of two uncorrelated[43] pairs. Detection of photons from uncorrelated pairs increases the noise, but does not influence the security of the key. Quite the contrary, for heralded single-photon sources all double pair emissions within the gate time of typically 1 ns offer a back door for the eavesdropper. Moreover, no random-number generator is required at all in entanglement-based quantum cryptography. In any case, our experiment might also be seen as a confirmation that a heralded single-photon source can operate successfully over such distances.

In this work, an optical ground station, developed for standard optical communication to and from satellites, has been adapted for use in quantum communication protocols. Various techniques, such as closed-loop tracking, were implemented to maintain a single-photon free-space link over 144 km between the two Canary Islands La Palma and Tenerife. The observed polarization correlation between the two observers violated the CHSH–Bell inequality by more than 13 standard deviations. The presence of entanglement was used to generate a quantum cryptographic key between La Palma and Tenerife. The distance between Alice and Bob exceeds that of previous experiments by an order of magnitude; this exploits the limit for ground-based free-space quantum communication. Significantly longer distances can be reached only using air- or space-based platforms. Our entangled-photon source was able to achieve coincidence production rates and fidelities to bridge readily the attenuation expected for a downlink from a low-Earth-orbit satellite to two different ground stations in future space experiments[25]. This experiment is an essential step towards future satellite-based distribution of quantum entanglement, to establish a worldwide network for quantum communication[24] and fundamental tests of quantum mechanics[44].

METHODS

In order to maintain our quantum communication link over sufficiently long timescales to make all necessary adjustments and measurements, we implemented an active stabilization of our optical link via a closed-loop tracking system, to correct the beam drifts induced by atmospheric changes. A green beacon laser was sent from the single-photon receiver on Tenerife to the single-photon transmitter on La Palma, that is, in the opposite direction to the quantum link. We used a divergent beacon laser with a spot size on La Palma of typically 100–200 m in diameter to ensure that the single-photon transmitter station was illuminated at all times. The beacon laser was focused by a separate tracking lens onto the tracking CCD (see Fig. 3). This enabled us to determine the angle of arrival (AOA) of the beacon laser compared with a

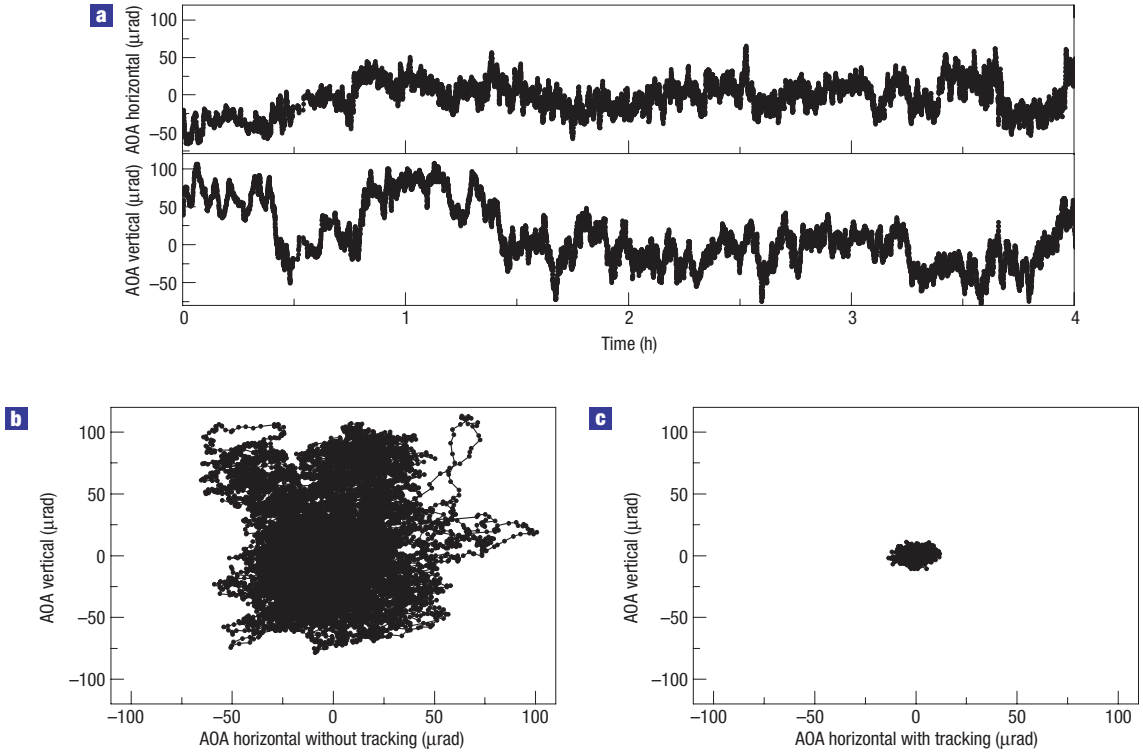

Figure 4 Long-term behaviour of the AOA of the tracking beacon on the tracking CCD. a, The horizontal (upper) and vertical (lower) movements of the single-photon transmitter telescope as a function of time over 4 h recorded with a repetition rate of about 1.2 Hz. Slow changes in average pointing direction occur owing to changes of the atmospheric gradients and layering. These data were taken with the tracking controller turned off. Note that the single-photon receiver aperture (1 m in diameter) corresponds to 7 μrad in the pointing direction of the single-photon-sender telescope. **b**, The data in an *x*–*y* scatter plot. The *x*–*y* position on the tracking CCD corresponds to an apparent location of the tracking beacon position depending on the optical path through the time-dependent atmospheric layers. Due to the fact that homogeneity of the atmosphere is stronger in the horizontal dimension, the beam is drifting higher in the vertical dimension. This can be compared to the dimensions of the OGS telescope aperture (1 m or 7 μrad) or a beam-drift of about 100 m on the single-photon receiver site to be 70 μrad. **c**, The difference from the predefined reference position is shown, now with closed-loop tracking which keeps the AOA of the centre of the single-photon beam in the required solid angle for the OGS telescope aperture.

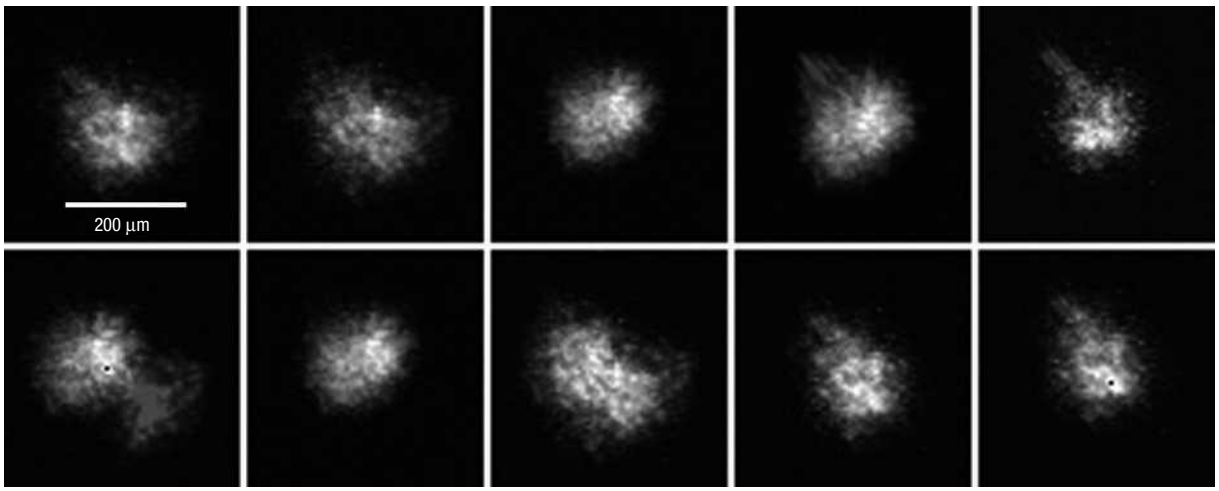

Figure 5 A time series of CCD images of the spot at the APDs illustrates the fluctuations due to atmospheric turbulence. The images were recorded with light from a laser diode and an integration time of 1 ms under good weather conditions. The spot size of 100–250 μm depending on weather conditions did not exceed the size of the detectors (500 μm).

reference pointing direction. The variations of the AOA were caused by changes of the atmospheric conditions in the optical path of the tracking beam on a timescale of tens of seconds to minutes (see Fig. 4). This can be seen as an apparent change of the position of the beacon laser at the OGS with respect to the transmitter station, consequently leading to a shift of the beacon's AOA on the tracking CCD. The difference between the measured and the predefined

AOA was used as an error signal for the closed-loop tracking system to maintain the pointing direction of the single-photon transmitter telescope automatically (Fig. 4c). This reference point was manually determined by optimizing the end-to-end transmission values on the quantum communication channel. The tracking optics set-up used an $f/4$ lens with $f = 400$ mm. Therefore, an alteration of the optical path corresponding to an apparent lateral shift of the OGS of 1 m induced over 144 km on La Palma an AOA change of 7 μrad and a 3 μm shift on the tracking CCD. Calculating the centre of the intensity distribution on the CCD (see Fig. 3), the spatial resolution of the tracking sensor was enhanced to 1 μm, or an AOA of 2.3 μrad. This means that the tracking sensor could pick up apparent lateral shifts of the OGS with a resolution of 33 cm. The error signal of the tracking sensor was fed into a closed proportional-control loop. To control the pointing direction of the telescope, stepper motors were used to move the telescope platform, with both the tracking and the single-photon transmitter optics attached to it.

Without tracking, the position of the focal point on the tracking CCD typically moved away from the reference point by three pixels within a couple of minutes, equivalent to a beam drift of approximately 4.5 m at the single-photon receiver site. Since the diameter of the single-photon beam is between 3 and 5 m on a night with reasonably good conditions, the spot of the single-photon beam completely moved away from the 1 m receiver aperture of the OGS telescope. As a consequence, the link attenuation decreased within a couple of minutes, typically from −30 to −45 dB (see Fig. 2). On the receiver side, the incoming beam had a 1.4° divergence. Atmospheric fluctuations implied a rapid (several kHz) transversal beam wander of about 3 mm on average in the focal plane of the Coudé focus (effective f-number of $f/38$) under moderate conditions. This corresponds to an average wavefront wander at the telescope aperture of 75 μrad. Therefore, a focal length reducer with an $f/5$ focusing system was implemented, reducing the average beam diameter to 420 μm to fit the silicon photodiode's (APD's) active area of 500 μm in diameter. The focal length reducer consisted of a collimating lens ($f = 400$ mm) routing the recollimated beam with a diameter of 10 mm through the polarization optics necessary for the experiment and of a focusing lens ($f = 50$ mm) to refocus the beam onto the detector. Figure 5 shows a time series of the spot at the APDs measured with an integration time of 1 s. The spot size was about 100 μm under good weather conditions and 400 μm under bad weather conditions. Interference filters with a full-width at half-maximum of 10 nm were used to suppress background light.

In order to test the polarization correlation of the photon pairs with the CHSH-type Bell inequality[36], it is necessary to determine the correlation function

$$E(\Phi_A, \Phi_B) = \frac{N_{++}(\Phi_A, \Phi_B) + N_{--}(\Phi_A, \Phi_B) - N_{+-}(\Phi_A, \Phi_B) - N_{-+}(\Phi_A, \Phi_B)}{N_{++}(\Phi_A, \Phi_B) + N_{--}(\Phi_A, \Phi_B) + N_{+-}(\Phi_A, \Phi_B) + N_{-+}(\Phi_A, \Phi_B)}$$

which was inferred from the measured coincidence counts $N_{ij}(\Phi_A, \Phi_B)$ for outcomes $\{i, j\}$ and polarization settings $\{\Phi_A, \Phi_B\}$ on Alice's and Bob's side, respectively, with $i, j \in \{+, -\}$, where $+$ and $-$ label the outputs of a two-channel polarization analyser (see Fig. 1). We conservatively estimated the error as the standard deviation of the poissonian count distribution. The correlation coefficients were combined to yield the value of the parameter S as

$$S = E(\Phi_A, \Phi_B) - E(\Phi_A, \Phi'_B) + E(\Phi'_A, \Phi_B) + E(\Phi'_A, \Phi'_B).$$

Here $\{\Phi_A, \Phi'_A\}$ and $\{\Phi_B, \Phi'_B\}$ are the measurement settings of Alice and Bob, respectively. According to the CHSH inequality, S is bound by $|S_{CHSH}| \leq 2$, whereas quantum mechanics predicts a violation of up to $S_{QM} = 2\sqrt{2} \approx 2.83$. This maximum is found for the polarization angles $(\Phi_A, \Phi'_A, \Phi_B, \Phi'_B) = (0°, 45°, 22.5°, 67.5°)$. We experimentally obtained the value $S_{Exp} = 2.508 \pm 0.037$ (see Table 1). Thereby, we violated the CHSH inequality by more than 13 standard deviations, proving the entanglement between the photons detected at the Canary Islands La Palma and Tenerife.

Received 3 July 2006; accepted 27 April 2007; published 3 June 2007.

References

1. Schroedinger, E. Die gegenwaertige Situation in der Quantenmechanik. *Die Naturwissenschaften* **49**, 823–828 (1935).
2. Einstein, A., Podolsky, B. & Rosen, N. Can quantum-mechanical description of physical reality be considered complete? *Phys. Rev.* **47**, 777–780 (1935).
3. Ekert, A. K. Quantum cryptography based on Bell's theorem. *Phys. Rev. Lett.* **67**, 661–663 (1991).
4. Bennett, C. H. & Brassard, G. *Proc. IEEE Int. Conf. on Computers, Systems and Signal Processing, Bangalore, India* 175–179 (IEEE, New York, 1984).
5. Jennewein, T. *et al.* Quantum cryptography with entangled photons. *Phys. Rev. Lett.* **84**, 4729–4732 (2000).
6. Bennett, C. H. *et al.* Teleporting an unknown quantum state via dual classical and EPR channels. *Phys. Rev. Lett.* **70**, 1895–1899 (1993).
7. Bouwmeester, D. *et al.* Experimental quantum teleportation. *Nature* **390**, 575–579 (1997).
8. Riebe, M. *et al.* Experimental quantum teleportation with atoms. *Nature* **429**, 734–737 (2004).
9. Barrett, M. D. *et al.* Deterministic quantum teleportation of atomic qubits. *Nature* **429**, 737–739 (2004).
10. Ursin, R. *et al.* Quantum teleportation link across the Danube. *Nature* **430**, 849 (2004).
11. Deutsch, D. & Ekert, A. Quantum computation. *Phys. World* **11**, 47–52 (1998).
12. Walther, P. *et al.* Experimental one-way quantum computing. *Nature* **434**, 169–176 (2005).
13. Prevedel, R. *et al.* High-speed linear optics quantum computing using active feed-forward. *Nature* **445**, 65–69 (2007).
14. Aspect, A., Dalibard, J. & Roger, G. Experimental test of Bell's inequalities using time-varying analyzers. *Phys. Rev. Lett.* **49**, 1804–1807 (1982).
15. Weihs, G., Jennewein, T., Simon, C., Weinfurter, H. & Zeilinger, A. Violation of Bell's inequality under strict Einstein locality conditions. *Phys. Rev. Lett.* **81**, 5039–5043 (1998).
16. Aspelmeyer, M. *et al.* Long-distance free-space distribution of entangled photons. *Science* **301**, 621–623 (2003).
17. Resch, K. J. *et al.* Distributing entanglement and single photons through an intra-city, free-space quantum channel. *Opt. Express* **13**, 202–209 (2005).
18. Peng, C.-Z. *et al.* Experimental free-space distribution of entangled photon pairs over a noisy ground atmosphere of 13 km. *Phys. Rev. Lett.* **94**, 150501 (2005).
19. Tittel, W. *et al.* Experimental demonstration of quantum correlations over more than 10 km. *Phys. Rev. A* **57**, 3229–3232 (1998).
20. Marcikic, I. *et al.* Distribution of time-bin entangled qubits over 50 km of optical fiber. *Phys. Rev. Lett.* **93**, 180502 (2004).
21. Takesue, H. *et al.* Differential phase shift quantum key distribution experiment over 105 km fibre. *New J. Phys.* **7**, 232 (2005).
22. Waks, E., Zeevi, A. & Yamamoto, Y. Security of quantum key distribution with entangled photons against individual attacks. *Phys. Rev. A* **65**, 52310 (2002).
23. Briegel, H.-J., Dür, W., Cirac, J. I. & Zoller, P. Quantum repeaters: The role of imperfect local operations in quantum communication. *Phys. Rev. Lett.* **81**, 5932–5935 (1998).
24. Nordholt, J. E., Hughes, R. J., Morgan, G. L., Peterson, C. G. & Wipf, C. C. Present and future quantum key distribution. *Proc. SPIE* **4635**, 116–126 (2002).
25. Kaltenbaek, R. *et al.* Proof-of-concept experiments for quantum physics in space. *Proc. SPIE Proc. Quantum Commun. Quantum Imaging* **5161**, 252–268 (2003).
26. Kwiat, P. G. *et al.* New high-intensity source of polarization-entangled photon pairs. *Phys. Rev. Lett.* **75**, 4337–4341 (1995).
27. Gisin, N., Ribordy, G., Tittel, W. & Zbinden, H. Quantum cryptography. *Rev. Mod. Phys.* **74**, 145–195 (2002).
28. Pfennigbauer, M. *et al.* Satellite-based quantum communication terminal employing state-of-the-art technology. *J. Opt. Netw.* **4**, 549–560 (2005).
29. Czichy, R. *et al.* Design of an optical ground station for in-orbit checkout of free space laser communication payloads. *SPIE* **2381**, 26–37 (1995).
30. Comeron, A. *et al.* Propagation experiments in the near infrared along a 150-km path and from stars in the Canarian archipelago. *Proc. SPIE* **4687**, 78–90 (2002).
31. Lange, R., Smutny, B., Wandernoth, B., Czichy, R. & Giggenbach, D. 142 km, 5.625 Gbps free-space optical link based on homodyne BPSK modulation. *Proc. SPIE* **6105**, 61050A1–61050A9 (2006).
32. Eltermann, L. UV, visible, and IR attenuation for altitudes to 50 km. *Environ. Res. Pap.* **285**, AFCRL–68–0153 (1968).
33. Kurtsiefer, C. *et al.* Quantum cryptography: A step towards global key distribution. *Nature* **419**, 450 (2002).
34. Hughes, R. J., Nordholt, J. E., Derkacs, D. & Peterson, C. G. Practical free-space quantum key distribution over 10 km in daylight and at night. *New J. Phys.* **4**, 43 (2002).
35. Fried, D. L. Statistics of a geometric representation of a wavefront distortion. *J. Opt. Soc. Am.* **55**, 1427–1435 (1965).
36. Clauser, J. F., Horne, M. A., Shimony, A. & Holt, R. A. Proposed experiment to test local hidden-variable theories. *Phys. Rev. Lett.* **23**, 880–884 (1969).
37. Bennett, C. H., Brassard, G. & Mermin, N. D. Quantum cryptography without Bell's theorem. *Phys. Rev. Lett.* **68**, 557–559 (1992).
38. Brassard, G. & Salvail, L. *EUROCRYPT '93: Workshop on the Theory and Application of Cryptographic Techniques on Advances in Cryptology* 410–423 (Lecture Notes in Computer Science, Vol. 765, Springer, New York, 1994).
39. Bennett, C. H., Brassard, G. & Robert, J. M. Privacy amplification by public discussion. *SIAM J. Comput.* **17**, 210–229 (1988).
40. Carter, J. L. & Wegman, M. N. Universal classes of hash functions. *J. Comput. Syst. Sci.* **19**, 143–154 (1979).
41. Wegman, M. N. & Carter, J. L. *Proc. 20th Ann. Symp. Found. Comput. Sci.* 175–182 (IEEE Computer Society, 1979).
42. Luetkenhaus, N. Security against individual attacks for realistic quantum key distribution. *Phys. Rev. A* **61**, 052304 (2000).
43. Weinfurter, H. & Zukowski, M. Four-photon entanglement from down-conversion. *Phys. Rev. A* **64**, 010102(R) (2001).
44. Bell, J. S. Free variables and local causality. *Dialectica* **39**, 103–106 (1985).

Acknowledgements

The authors wish to thank F. Sanchez (Director IAC) and A. Alonso (IAC), T. Augusteijn and the staff of the Nordic Optical Telescope (NOT) and the staff of the Telescopio Nazionale Galileo (TNG) in La Palma for their support at the trial sites. Furthermore, we thank C. Brukner and J. Kofler for helpful discussions. This work was supported by ESA under the General Studies Programme (QIPS study, ESA contract number 18805/04/NL/HE), the Austrian Science Foundation (FWF) under project number SFB1520, the A8-Quantum information Highway project of the Bavarian High-Tech Initiative, the European projects SECOQC and QAP and the ASAP programme of the Austrian Space Agency (FFG). Additional support was provided by the ESA, the Swiss National Science Foundation (SNF) and the DOC program of the Austrian Academy of Sciences.
Correspondence and requests for materials should be addressed to R.U. or A.Z.

Competing financial interests

The authors declare no competing financial interests.